

SIMBa: System Identification Methods leveraging Backpropagation

Loris Di Natale,[†] Muhammad Zakwan,[†] Philipp Heer, Giancarlo Ferrari Trecate, Colin N. Jones

Abstract—This manuscript details the SIMBa toolbox (System Identification Methods leveraging Backpropagation), which uses well-established Machine Learning tools for discrete-time linear multi-step-ahead state-space System Identification (SI). Backed up by novel linear-matrix-inequality-based free parametrizations of Schur matrices to guarantee the stability of the identified model *by design*, SIMBa allows for seamless integration of prior system knowledge. In particular, it can simultaneously enforce desired system properties — such as sparsity patterns — and stability on the model, solving an open SI problem.

We extensively investigate SIMBa’s behavior when identifying diverse systems with various properties from both simulated and real-world data. Overall, we find it consistently outperforms traditional stable subspace identification methods, and sometimes significantly, even while enforcing desired model properties. These results hint at the potential of SIMBa to pave the way for generic structured nonlinear SI. The toolbox is open-sourced on <https://github.com/Cemempamoi/simba>.

Index Terms—Backpropagation, Discrete LTI Systems, Grey-box modeling, Machine Learning, System Identification, Toolbox.

I. INTRODUCTION

NEURAL Networks (NNs) recently gained a lot of attention, achieving impressive performance on a wide variety of tasks [1], [2]. Consequently, they have been used for nonlinear System Identification (SI) tasks, where they have also attained state-of-the-art performance [3]–[5]. While NNs can model complex nonlinearities, they might perform sub-optimally in cases where the structure of the system is known, such as for *linear* systems, where traditional SI methods [6] perform well [7].

On the other hand, as demonstrated in [8], one can leverage the Automatic Differentiation (AD) techniques at the core of NN training to improve upon traditional stable linear SI methods. Relying on the efficient and open-source `PyTorch` Python library [9] and a free parametrization of Schur matrices, SIMBa [8] indeed showed significant performance gains compared to traditional stable SI implementations in MATLAB [10] and Python [11].

In this work, we extend the open-source SIMBa (System Identification Methods leveraging Backpropagation) toolbox

originally presented in [8] beyond standard stability guarantees, allowing for more general *prior knowledge integration*. Specifically, we show how SIMBa can incorporate structures in the state-space matrices to identify, for example, to enforce desired sparsity patterns. This information might indeed be known to the user *a priori*: one may have insights on which states are measured, which inputs impact which states, or which states exchange information, i.e., the topology of a networked system, among others.

A. Traditional linear system identification

Traditionally, input-output state-space models are identified through Subspace Identification Methods (SIMs) [12]. Remarkably, N4SID [13], MOESP [14] and CVA [15] have later been unified under a single theory in [16], proving they rely on similar concepts. In addition to these classical SIMs, *parsimonious* SIMs (PARSIMs) were introduced more recently to guarantee the causality of the identified models. While PARSIM-S [17] and PARSIM-P [18] assume no correlation between the input and the output noise, PARSIM-K [19] was later developed for closed-loop SI.

When stability is desired, *post-hoc* corrections can be applied to the state-space matrices identified by SIMs to obtain a stable model [20]. However, this is impossible for PARSIMs and might cause severe performance drops on traditional SIMs [11]. Alternatively, one can rewrite the Least Squares (LS) optimization at the heart of SIMs as a constrained optimization problem that ensures stability [21], [22]. Similarly, one may leverage parametrization of Schur matrices [23], [24] to guarantee the stability of the identified system through projected Gradient Descent (GD), for example [25].

B. Prior knowledge integration

In addition to maintaining the stability of the system, it can be beneficial, and sometimes necessary, to convey expert knowledge or desired properties to the identified model in practice. This led to the development of SIMs specifically tailored for distributed systems with different topologies, for example, where the state-space matrices are known to have specific sparsity patterns [26]–[29].

More generally, an expert might have prior knowledge about the structure of the system stemming from known physical properties, for example. To ensure the identified model follows the desired dynamics, one typically writes down the corresponding state and output equations manually and then identifies the unknown parameters from data. Such *grey-box* modeling approaches have been successfully applied to

This research was supported by the Swiss National Science Foundation under NCCR Automation, grant agreement 51NF40_180545.

L. Di Natale and P. Heer are with the Urban Energy Systems Laboratory, Swiss Federal Laboratories for Materials Science and Technology (Empa), 8600 Dübendorf, Switzerland. L. Di Natale, M. Zakwan, G. Ferrari Trecate, and C.N. Jones are with the Laboratoire d’Automatique, Swiss Federal Institute of Technology Lausanne (EPFL), 1015 Lausanne, Switzerland.

[†] L. Di Natale and M. Zakwan contributed equally to this work. Corresponding author: L. Di Natale, loris.dinatale@alumni.epfl.ch.

building [30], chemical process [31], or robotic system [32] modeling, among others.

These considerations were recently unified in the COSMOS framework, which allows one to identify structured linear systems from input-output data [33]. It is based on rewriting the LS estimate in SIMs as a rank-constrained optimization problem to ensure the identified matrices belong to the desired parametrized sets. However, COSMOS minimizes the one-step-ahead prediction error and does not guarantee the stability of the identified model.

We note here that knowledge integration also encompasses the careful initialization of all the parameters, which has already been shown to improve performance in the context of nonlinear SI [34]. While this is not needed for classical subspace methods, which rely on deterministic LS solutions [12], it can have a significant impact on the convergence rate and quality of the solutions of gradient-based algorithms [35]. This was already observed for SIMBa in [8].

C. Contribution

None of the aforementioned methods allowing prior knowledge integration considered the stability of the resulting model. Additionally, they usually rely on one-step-ahead fitting criteria. To the best of the authors' knowledge, simultaneously imposing sparsity or other desired properties *and* stability constraints with multi-step-ahead identification is still an open problem that we propose to solve in this paper.

To achieve this, we extend SIMBa to let one incorporate desired system properties without jeopardizing the stability of the identified model. Leveraging novel free parameterizations of Schur matrices and well-established ML tools for multi-step prediction error minimization, we show how SIMBa can clearly outperform traditional SI methods. To this end, we conduct extensive numerical experiments, identifying different systems with and without state measurements, from simulated as well as real-world data, and while enforcing various system properties.

SIMBa incurs large computational burdens, requiring from several minutes to over an hour for training, in contrast to the few seconds needed for conventional methods. However, it consistently — and sometimes significantly — outperforms traditional approaches on a wide variety of problems in terms of accuracy, even while enforcing desired properties. SIMBa could hence be very beneficial in applications where performance is critical or system properties must be respected.

Together, these investigations hint at the efficacy of ML tools to improve upon traditional methods and pave the way for a generic nonlinear SI framework. Indeed, SIMBa could integrate nonlinearities, similarly to [36], [37], or be fused in Koopman-based approaches like [38]–[41] to enforce stability.

Organization: After a few preliminaries in Section II, Section III presents the main theoretical results on the free parametrization of Schur matrices. Section IV then introduces the SIMBa toolbox in detail and Section V provides extensive numerical validations and analyses. Finally, Section VI discusses some limitations and potential extensions of SIMBa before Section VII concludes the paper.

II. PRELIMINARIES

This work is concerned with the identification of discrete-time linear time-invariant state-space models of the form

$$x_{k+1} = Ax_k + Bu_k \quad (1a)$$

$$y_k = Cx_k + Du_k, \quad (1b)$$

where $x \in \mathbb{R}^n$, $u \in \mathbb{R}^m$, $y \in \mathbb{R}^p$ are the states, inputs, and outputs, respectively. The objective is to identify $A \in \mathbb{R}^{n \times n}$, $B \in \mathbb{R}^{n \times m}$, $C \in \mathbb{R}^{p \times n}$, and $D \in \mathbb{R}^{p \times m}$ from data.

To that end, throughout this work, we assume access to a data set $\mathcal{D}^{i/o} = \{(u(0), y(0)), \dots, (u(l_s), y(l_s))\}_{s=1}^N$ of N input-output measurement trajectories s of length l_s . Note that, in some cases, one might have direct access to state measurements, in which case (1b) is omitted and only A and B need to be identified from a data set of input-state measurements $\mathcal{D}^{i/s} = \{(u(0), x(0)), \dots, (u(l_s), x(l_s))\}_{s=1}^N$. In our experiments, we split the data into a training, a validation, and a test set of trajectories \mathcal{D}_{train} , \mathcal{D}_{val} , and \mathcal{D}_{test} , respectively, as often done in ML pipelines [42].

When we want to enforce the asymptotic stability of (1), we need to ensure A is Schur, i.e., all its eigenvalues $\lambda_i(A)$ satisfy $|\lambda_i(A)| < 1, \forall i = 1, \dots, n$ [43].

Finally, given a matrix $M \in \mathbb{R}^{q \times s}$, the *binary mask* $\text{sparse}(M) := \mathcal{M} \in \{0, 1\}^{q \times s}$ represents its *sparsity pattern*. Such a sparse matrix can be written as $M := \mathcal{M} \odot \bar{M}$, with \bar{M} a matrix of appropriate dimensions and \odot the Hadamard product between two matrices.

Notation: Let \mathbb{I}_q and $\mathbb{1}_{q \times q}$ be the identity and all-one matrix of dimension q , respectively. Given a matrix $H \in \mathbb{R}^{2q \times 2q}$, we define its block components $H_{11}, H_{12}, H_{21}, H_{22} \in \mathbb{R}^{q \times q}$ as

$$\begin{bmatrix} H_{11} & H_{12} \\ H_{21} & H_{22} \end{bmatrix} := H. \quad (2)$$

For a symmetric matrix $F \in \mathbb{R}^{q \times q}$, $F \succ 0$ means it is positive definite. For a generic matrix $J \in \mathbb{R}^{q \times q}$, $\lambda_{\min}(J)$ and $\lambda_{\max}(J)$ refer to its minimum and maximum eigenvalue, respectively, and

$$|\lambda(J)|_{\max} := \max_{i=1, \dots, n} |\lambda_i(J)|$$

to its maximum absolute eigenvalue. Finally, $\sigma := \mathbb{R} \rightarrow]0, 1[$ corresponds to the sigmoid function, i.e., $\sigma(r) = (1 + e^{-r})^{-1}$, σ^{-1} to its inverse, and $\|\cdot\|_p$ to the p -norm of a vector.

III. FREE PARAMETRIZATIONS OF SCHUR MATRICES

To efficiently leverage PyTorch's automatic differentiation framework — which cannot deal with constrained optimization — for stable SI tasks, we require A to be Schur *by design*. This will then allow us to run unconstrained Gradient Descent (GD) in the search space without jeopardizing the stability of the identified system. Inspired by [44], we leverage Linear Matrix Inequalities (LMIs) to design matrices that simultaneously guarantee stability and capture various system properties.¹

¹Except for Proposition 4, which relies on different arguments.

A. Dense Schur matrices

For completeness, let us first state a slightly modified version of the free parametrization proposed and proved in [8], which characterizes Schur matrices with an arbitrary structure.

Proposition 1. *For any $W \in \mathbb{R}^{2n \times 2n}$, $V \in \mathbb{R}^{n \times n}$, $0 < \gamma \leq 1$, and $\epsilon > 0$, let*

$$S := W^\top W + \epsilon \mathbb{I}_{2n}. \quad (3)$$

Then

$$A = S_{12} \left[\frac{1}{2} \left(\frac{S_{11}}{\gamma^2} + S_{22} \right) + V - V^\top \right]^{-1} \quad (4)$$

is Schur with $|\lambda_i(A)| < \gamma, \forall i = 1, \dots, n$.

Note that γ is a user-defined parameter bounding the eigenvalues of A in a circle of the corresponding radius centered at the origin, potentially enforcing desired system properties on the learned matrix. This parametrization has been shown to capture *all* Schur matrices A when $\epsilon = \epsilon(A)$ is adapted during training [8, Remark 1]. This can, however, lead to numerical instabilities in practice if ϵ takes excessively small values and we hence fix it to a small arbitrary constant in our implementations. Critically, it does not hinder the representation power of Proposition 1, which can still capture all Schur matrices, as detailed in the following corollary.

Corollary 1. *For any given Schur matrix A and $\epsilon > 0$, there exists $W \in \mathbb{R}^{2n \times 2n}$, $V \in \mathbb{R}^{n \times n}$ satisfying (4) for S as in (3).*

Proof. See Appendix A. \square

B. Discretized continuous-time systems

Many linearized real-world systems are continuous-time, i.e., of the form

$$\dot{x} = \bar{A}x + \bar{B}u \quad (5a)$$

$$\dot{y} = Cx + Du. \quad (5b)$$

After a forward Euler discretization, (5) becomes

$$\begin{aligned} x_{k+1} &= (\mathbb{I}_n + \delta \bar{A}) x_k + \delta \bar{B} u_k \\ y_k &= C x_k + D u_k, \end{aligned}$$

where $\delta > 0$ is the discretization step.² In particular, the matrix A we want to identify from discrete-time data samples while ensuring stability now takes the form

$$A := \mathbb{I}_n + \delta \bar{A}. \quad (6)$$

In other words, if the data in $\mathcal{D}^{i/o}$ or $\mathcal{D}^{i/s}$ has been collected from a continuous-time system, then A will be *close to identity*. Note that a similar behavior would also be expected from slow-changing systems. The following proposition offers a parametrization of A that takes this structure into account.

Proposition 2. *For any $W \in \mathbb{R}^{2n \times 2n}$, $V \in \mathbb{R}^{n \times n}$, and $\epsilon > 0$, let*

$$S := W^\top W + \epsilon \mathbb{I}_{2n}. \quad (7)$$

²While different discretization schemes exist, we focus on the forward Euler one herein as it allows us to derive another meaningful parametrization of Schur matrices.

Then

$$A = \mathbb{I}_n - 2 (S_{11} + V - V^\top)^{-1} S_{12} S_{22}^{-1} S_{21} \quad (8)$$

is a Schur matrix.

Proof. See Appendix B. \square

Contrary to Proposition 1 and as evident from (8), the matrix A will be steered towards the identity matrix here, as desired. If the given data stems from a continuous-time or slow-changing discrete-time system, this might ease SIMBa's learning procedure, and we will leverage it in Section V-D. Importantly, Proposition 2 does not sacrifice any representation power, as demonstrated in the following corollary.

Corollary 2. *For any given Schur matrix A and $\epsilon > 0$, there exists $W \in \mathbb{R}^{2n \times 2n}$, $V \in \mathbb{R}^{n \times n}$ satisfying (8) for S as in (7).*

Proof. See Appendix C. \square

Remark 1. *The discretization step δ does not appear in (8). While it might seem counter-intuitive at first glance, this is not an issue in practice: changing the discretization step would indeed modify the data collection for $\mathcal{D}^{i/o}$ or $\mathcal{D}^{i/s}$, thereby naturally changing the solution found by SIMBa through GD and hence the form of A . In other words, A does implicitly depend on δ , as expected.*

C. Sparse Schur matrices

Let us now assume the sparsity pattern \mathcal{M} of A is given. This might arise in cases where the system to identify is a networked system with a known topology, for example. The following proposition shows one possibility to parameterize such sparse matrices without losing stability guarantees.

Proposition 3. *For a given sparsity pattern $\mathcal{M} \in \{0, 1\}^{n \times n}$, any $W \in \mathbb{R}^{2n \times 2n}$, $V \in \mathbb{R}^{n \times n}$, and $\epsilon > 0$, let*

$$S := W^\top W + \epsilon \mathbb{I}_{2n} \quad (9)$$

and construct the diagonal matrix N with entries

$$N_{ii} := \max \left\{ \sum_{j \neq i} \mathcal{M}_{ij}, \sum_{j \neq i} \mathcal{M}_{ji} \right\} + \epsilon, \quad \forall i = 1, \dots, n. \quad (10)$$

Then, the matrix

$$A = \mathcal{M} \odot \left(S_{12} \left[N \odot \left(\frac{1}{2} (S_{11} + S_{22}) + V - V^\top \right) \right]^{-1} \right) \quad (11)$$

is Schur and presents the desired sparsity pattern \mathcal{M} .

Proof. See Appendix D. \square

For a given sparsity pattern \mathcal{M} and small positive constant ϵ , one can thus define N and use the free parametrization (11) to compute Schur matrices presenting the desired sparsity pattern from some V and W .

Remark 2. *Contrary to Propositions 1 and 2, Proposition 3 is conservative; it cannot capture all sparse Schur matrices. This stems from two steps in Appendix D. First, we have to restrict our search to systems admitting diagonal Lyapunov*

functions to leverage the associative property of Hadamard products with diagonal matrices. Second, satisfying (27)–(28) is only a sufficient condition for (26) to hold.

Remark 3. Setting $\mathcal{M} := \mathbb{1}_{n \times n}$ would provide another parametrization of dense Schur matrices, potentially replacing Proposition 1. However, this is not advised in practice since (11) is more conservative than (4) (see Remark 2).

D. An alternative general parametrization

To showcase the power of PyTorch, which can differentiate through the computation of eigenvalues, the following proposition offers an alternative free parametrization of any Schur matrix. Contrary to the other parametrizations, it relies on scaling arguments instead of LMIs.

Proposition 4. For a given sparsity pattern $\mathcal{M} \in \{0, 1\}^{n \times n}$, $0 < \gamma \leq 1$, and any matrix $V \in \mathbb{R}^{n \times n}$ and constant $\eta \in \mathbb{R}$, leveraging the sigmoid function σ , the matrix

$$A = \frac{\sigma(\eta)\gamma}{|\lambda(\mathcal{M} \odot V)|_{\max}} (\mathcal{M} \odot V) \quad (12)$$

is Schur with $|\lambda_i(A)| < \gamma, \forall i = 1, \dots, n$, and presents the desired sparsity pattern \mathcal{M} .

Proof. See Appendix E. \square

As can be seen, Propositions 3 and 4 can be used interchangeably; they both provide a free parametrization of sparse and stable matrices. Contrary to its conservative counterpart, however, Proposition 4 can capture *all* Schur matrices – including sparse ones –, as shown in the following corollary.

Corollary 3. Any Schur matrix A satisfies (12) for some $\mathcal{M} \in \{0, 1\}^{n \times n}$, $0 < \gamma \leq 1$, $V \in \mathbb{R}^{n \times n}$, and $\eta \in \mathbb{R}$.

Proof. One can set $\mathcal{M} := \text{sparse}(A)$, $V := A$, γ such that $|\lambda(A)|_{\max} < \gamma \leq 1$, which exists since the matrix A is Schur, and $\eta := \sigma^{-1}(|\lambda(A)|_{\max}/\gamma)$, which is well-defined since $|\lambda(A)|_{\max}/\gamma < 1$ by definition of γ . \square

Interestingly, defining $\mathcal{M} := \mathbb{1}_{n \times n}$ in Proposition 4, we recover a free parametrization of generic matrices, providing an alternative to Proposition 1. However, according to Corollary 3, this would not come at the cost of expressiveness, contrary to Proposition 3. Similarly, parametrizing V as in (6) and using $\mathcal{M} := \mathbb{1}_{n \times n}$, we recover a parametrization of matrices close to identity interchangeable with Proposition 2. Overall, Proposition 4 hence allows us to characterize *any* type of Schur matrix discussed throughout this Section.

Remark 4. Proposition 4 is conceptually related to [45], where a Lyapunov function is learned simultaneously to nominal system dynamics. At each step, the dynamics are then projected onto the Lyapunov function to guarantee asymptotic stability. Similarly, (12) can be seen as a projection onto some (unknown) Lyapunov function. However, the latter is implicitly defined through the scaling of A instead of being learned, hence alleviating the associated computational burden.

Remark 5. Leveraging techniques similar to [46], Propositions 1 and 3 can be adapted for continuous-time systems of

```
## Import SIMBa and the default parameters
from simba.model import Simba
from simba.parameters import base_parameters as parameters

## Prepare the data (unused data can be set to None,
# e.g., X for input-output systems)
U, X, Y, x0 = train_data
U_val, X_val, Y_val, x0_val = validation_data
U_test, X_test, Y_test, x0_test = test_data

## Customize the parameters to the problem
parameters['input_output'] = True
# ...

## Declare Simba, train it, and save the results
simba = Simba(nx=nx, nu=nu, ny=ny, parameters=parameters)
simba.fit(U, U_val, U_test, X, X_val, X_test,
         Y, Y_val, Y_test, x0, x0_val, x0_test)
simba.save(directory=directory, save_name=save_name)
```

Fig. 1. Main steps of running SIMBa in Python.

the form (5). On the other hand, the scaling approach deployed in Proposition 4 to control the magnitude of the eigenvalues of A cannot be straightforwardly adapted to the continuous-time setting, where the real part of each eigenvalue has to be negative to ensure stability.

E. Using free parametrizations

Propositions 1–4 imply one can choose *any* $\epsilon > 0$, $0 < \gamma \leq 1$, $\mathcal{M} \in \{0, 1\}^{n \times n}$, $V \in \mathbb{R}^{n \times n}$, $W \in \mathbb{R}^{2n \times 2n}$, and $\eta \in \mathbb{R}$ — depending on the setting — and construct a stable matrix A as in (4), (8), (11), or (12). In practice, ϵ should be set to a small constant³ and γ and \mathcal{M} are problem-specific and user-defined since they stem from prior knowledge about the system. Therefore, all *constrained* parameters are defined by the user *a priori*.

SIMBa then searches for V , W , and η optimizing some performance criterion as detailed in Section IV. Since these parameters are *not* constrained, we can use unconstrained GD for this task. Propositions 1–4 hence allow us to leverage the full power of PyTorch to fit the data without jeopardizing stability, constructing a Schur matrix A from the *free* parameters V , W , and η at every iteration.

IV. THE SIMBA TOOLBOX

This Section describes the main parameters of SIMBa, restating the ones discussed in [8] for completeness, introducing new ones pertaining to prior knowledge integration, and discussing critical hyperparameters in more detail. SIMBa is implemented in Python to leverage the efficient AD framework of PyTorch [9] and open-sourced on <https://github.com/Cemempamoi/simba>. For given data sets $\mathcal{D}_{\text{train}}$, \mathcal{D}_{val} , and $\mathcal{D}_{\text{test}}$, SIMBa can be initialized, fit, and saved in a few lines of codes, as exemplified in Fig. 1. We also provide a MATLAB interface inspired by the traditional MATLAB SI toolbox [10], as shown in Fig. 2.

³We use $\epsilon = 1\text{e-}6$ in our experiments.

```

%% Prepare the data
data = iddata(Y, U, Ts);
data_val = iddata(Y_val, U_val, Ts);
data_test = iddata(Y_test, U_test, Ts);

% Set paths to Python virtual env and Simba's main directory
path_to_python_env = fullfile('..', '.venv', 'bin', 'python');
path_to_simba = '..';

%% Launch python and load default options
[pe, opt] = SIMBaOptions(path_to_python_env, path_to_simba);
% Modify parameters (some of them are required)
opt.delta = 'None';
opt.input_output = true;
% ...

%% Run SIMBa
sys = run_simba(opt, data, data_val, data_test, Ts);

```

Fig. 2. Main steps to call SIMBa from MATLAB.

A. Optimization framework

Given input-output data $\mathcal{D}^{i/o}$, SIMBa iteratively runs gradient descent on batches of trajectories $Z \in \mathcal{D}_{train}$ randomly sampled from the training data set — thus seamlessly handling training data sets consisting of several trajectories — to solve the following optimization problem:

$$\min_{A, B, C, D, x_0^{(s)}} \frac{1}{|Z|} \sum_{s \in Z} \left[\frac{1}{l_s} \sum_{k=0}^{l_s} m_k^{(s)} \mathcal{L}_{train} \left(y^{(s)}(k), y_k^{(s)} \right) \right] \quad (13)$$

$$\text{s.t. } y_k^{(s)} = Cx_k^{(s)} + Du^{(s)}(k) \quad (14)$$

$$x_{k+1}^{(s)} = Ax_k^{(s)} + Bu^{(s)}(k). \quad (15)$$

In words, SIMBa minimizes the multi-step-ahead prediction error, using the training loss \mathcal{L}_{train} as performance criterion. In this paper, we rely on the Mean Squared Error (MSE), i.e., $\mathcal{L}_{train}(y, \hat{y}) = \|y - \hat{y}\|_2^2$. However, SIMBa's flexibility — backed by PyTorch's ability to handle any differentiable function — allows one to design custom (differentiable) loss functions and pass them through the `train_loss` parameter. In some applications, it might for example be interesting to optimize the Mean Absolute Error (MAE) or the Mean Absolute Percentage Error (MAPE), which are respectively more robust against outliers or different output magnitudes.

In many cases, identifying the matrix D is not required, which is achieved in SIMBa by setting `id_D=False`, removing the second term of (14). Similarly, if $x^{(s)}(0)$ is known, `learn_x0` can be toggled to `False` and SIMBa will fix $x_0^{(s)} := x^{(s)}(0)$ instead of optimizing it. The number of sequences $|Z|$ used for each gradient update can be controlled through the `batch_size` parameter.

Finally, $m_k^{(s)} \in \{0, 1\}$ in (13), with

$$m_k^{(s)} = \begin{cases} 0, & \text{with probability } p \text{ or if } y^{(s)}(k) \text{ is NaN,} \\ 1, & \text{otherwise.} \end{cases}$$

In words, these binary variables let SIMBa discard missing values from the objective function, allowing it to seamlessly work with incomplete data sets. Additionally, the user can define a `dropout = p` parameter to randomly remove

data points from the objective with probability p , providing empirical robustness to the training procedure. Indeed, it can be seen as a means to avoid overfitting the training data.

B. Input-state identification

When state measurements are available in $\mathcal{D}^{i/s}$, one can set `input_output=False`, dropping (14), and modifying the objective to

$$\min_{A, B} \frac{1}{|Z|} \sum_{s \in Z} \left[\frac{1}{l_s} \sum_{k=0}^{l_s} m_k^{(s)} \mathcal{L}_{train} \left(x^{(s)}(k), x_k^{(s)} \right) \right]. \quad (16)$$

Furthermore, for autonomous systems, the autonomous flag can be toggled, in which case the minimization on B is also discarded, as well as the corresponding second term on the right-hand-side of (15). Similarly to Section IV-A, $m_k^{(s)}$ are binary variables that can be forced to zero either to discard missing values or as a means of regularization.

Since the state x is known, one can break given training trajectories into *segments* of length `horizon`. The `stride` defines how many steps should be taken between the *starts* of two segments. Note that if `stride` is smaller than `horizon`, then segments of data will overlap, i.e., data points will appear several times in consecutive segments. If the user is interested in the model performance over a specific horizon length, this can be specified with `horizon_val`, and the number of segments can also be controlled with `stride_val`. Note that setting `horizon` or `horizon_val` to `None` keeps entire trajectories.

C. Training procedure

SIMBa iteratively runs one step of gradient descent on (13) or (16) for `max_epochs` epochs. Here, we define an *epoch* as one pass through the training data, i.e., every trajectory has been drawn in a batch Z . After each epoch, the validation data is used to assess the current model performance by computing

$$\frac{1}{|\mathcal{D}_{val}|} \sum_{s \in \mathcal{D}_{val}} \left[\frac{1}{l_s} \sum_{k=0}^{l_s} \mathcal{L}_{val} \left(y^{(s)}(k), y_k^{(s)} \right) \right],$$

replacing outputs by states when measurements are available. This evaluation metric is used to avoid SIMBa overfitting the training data: the best parameters, stored in memory, are only overwritten if the current parameters improve the performance on the validation set, and not the training one [42]. At the end of the training, to get a better estimate of the true performance of the identified model, we evaluate it on the unseen test data:

$$\frac{1}{|\mathcal{D}_{test}|} \sum_{s \in \mathcal{D}_{test}} \left[\frac{1}{l_s} \sum_{k=0}^{l_s} \mathcal{L}_{val} \left(y^{(s)}(k), y_k^{(s)} \right) \right],$$

similarly substituting outputs by states when measurements are available. Throughout this work, we also rely on the MSE for validation and testing, setting $\mathcal{L}_{val} = \mathcal{L}_{train}$, but this can be modified through the `val_loss` parameter. This gives the users the freedom to evaluate SIMBa on a different metric than the training one. It can be tailored to specific applications: SIMBa would then return the model performing best with

respect to the chosen evaluation criterion, irrespective of the training procedure.

Note that (13) or (16) can be highly nonconvex, in which case gradient descent cannot be expected to find the global optimum and will most likely settle in a local one instead. SIMBa is thus sensitive to its initialization and some hyperparameters and might converge to very different solutions depending on these choices.

D. Initialization

To start SIMBa in a relevant part of the search space, the user can toggle `init_from_matlab_or_ls` parameter to `True`. This prompts SIMBa to a run traditional SI method, i.e., either

- the MATLAB SI toolbox [10] or the Python SIPPY package [11] for input-output systems,⁴ or
- a traditional LS optimization in the input-state case,

before training. Depending on the setting, the chosen *initialization method* returns matrices A^* , and potentially B^* , C^* , and D^* . These are then used as initial choices of state-space matrices in SIMBa, so that it starts learning from the best solution found by traditional SI methods.

However, to ensure the often-desired stability of A , SIMBa relies on the free parameterizations in Propositions 1–4, in which case it is not possible to directly initialize A to A^* . We thus again resort to PyTorch to approximate it by solving the following optimization problem with unconstrained GD:

$$\min_{W, V, \eta} \mathcal{L}_{init}(A, A^*) \quad (17)$$

$$\text{s.t. } A \text{ as in (4), (8), (11), or (12)}, \quad (18)$$

with \mathcal{L}_{init} the desired loss function. We use the MSE throughout our numerical experiments but custom functions can be passed through the `init_loss` parameter.

Similarly to what was mentioned in Section IV-C concerning SIMBa’s training, this procedure is not guaranteed to find the global optimal solution, i.e., to converge to A^* . Consequently, even initialized instances of SIMBa might perform very differently from the initialization method, sometimes incurring large performance drops. Nonetheless, throughout our experiments, it usually worked well, finding an A close to A^* , as long as no prior system knowledge is available.

Indeed, since desired system properties cannot be enforced on traditional SI methods, the initialization method will always return dense and generic state-space matrices. In that case, SIMBa would try to match matrices following the required patterns to these generic matrices, which might lead to poor solutions. It is hence not advised to use `init_from_matlab_or_ls` when prior system knowledge is available; one should rather directly enforce this knowledge on SIMBa and let it learn from scratch.

Remark 6. *Note that A might be initialized exactly in the specific case when Proposition 4 is leveraged for stability and $\gamma > |\lambda(A^*)|_{\max}$, as detailed in the proof of Corollary 3. On*

the other hand, although Corollaries 1–2 demonstrate that any Schur matrix A^ can be parametrized as (4) or (8), respectively, they only show the existence of such a parametrization and cannot be used in practice to construct it.*

E. Prior knowledge integration

If certain sparsity patterns are desired for A , B , C , or D , they can be passed through `mask_{X}`, replacing $\{X\}$ with the name of the corresponding matrices. If the mask of B is given as \mathcal{M}_B , for example, (15) is modified to

$$x_{k+1}^{(s)} = Ax_k^{(s)} + (\mathcal{M}_B \odot B)u^{(s)}(k) \quad (19)$$

to force the desired entries of B to zero while letting SIMBa learn the others.

Similarly, `{X}_init` is used to initialize a given matrix to a specific value, and `learn_{X}=False` drops the corresponding matrix from the optimization, fixing it at its initial value. To control the magnitude of the eigenvalues of A in the free parameterizations of Propositions 1 and 4, one can set `max_eigenvalue = γ` .

Finally, `stable_A=True` enforces the stability of A : setting `naive_A=True` leverages Proposition 4 while toggling `LMI_A` uses Propositions 1–3. Specifically, if `delta` is not `None` but takes the value δ , hinting we are expecting A to be close to the identity matrix, then Proposition 2 is used instead of Proposition 1. Similarly, if `mask_A` is not `None`, hence requiring a sparse system, Proposition 3 is leveraged.

When `stable_A=True`, the minimization over A in (13) or (16) is replaced by a minimization over W , V , and/or η — depending on which of the four Propositions is used — and constraint (18) is added to the corresponding optimization problem.

F. Tuning of critical hyperparameters

As for NNs, which heavily rely on the same backpropagation backbone, the `learning_rate` is an important parameter: too large values lead to unstable training while too small ones slow the convergence speed. In general, throughout our empirical analyses, the default value of $1e-3$ showed very robust performance, and we couple it with a high number of epochs to ensure SIMBa can converge close to a local minimizer. However, this is problem-dependent, and the rate might be increased to accelerate learning if no instability is observed. Similarly, `init_learning_rate` controls the learning rate of the initialization in (17)–(18) when required. It also defaults to $1e-3$ due to its robust performance when coupled with a high number of `init_epochs`.

To further promote stable learning behaviors, we implemented a gradient clipping operation, pointwise saturating the gradients of all the parameters to avoid taking too large update steps during GD. These can be controlled through `grad_clip` and `init_grad_clip` during the training and the initialization phase, respectively. The default values of 100, respectively 0.1, were empirically tuned to achieve good performance. Although it might come at the cost of a slower convergence, our numerical investigations showed gradient clipping can significantly improve the quality of the solution found by SIMBa.

⁴Since several traditional SI methods are available, SIMBa uses the one achieving the best performance on the validation set.

V. NUMERICAL EXPERIMENTS

As described in Section IV, SIMBa can identify models from input-output and input-state measurements while seamlessly enforcing desired system properties such as stability or sparsity patterns. This Section provides numerical examples showcasing its ability to outperform traditional SI methods in a wide variety of case studies. It exemplifies how SIMBa can leverage Propositions 1–4 to guarantee the stability of the identified model while achieving state-of-the-art fitting performance. Interestingly, our investigations hint that integrating prior knowledge, while being easy, does not impact the quality of the solution found by SIMBa in general. On the contrary, it seems that domain knowledge injection can be helpful to improve performance.

Sections V-A–V-C first analyze the behavior of SIMBa on different simulated input-output data sets, complementing the results obtained in [8]. Throughout these experiments, we fixed $x_0 = 0$, which allows us to compare SIMBa with SIPPY’s implementations of SIMs and PARSIMs [11].⁵ We then investigate the performance of SIMBa on an input-state identification task from real-world measurements in Section V-D. We show how SIMBa surpassed the standard LS method and the state-of-the-art SOC approach for stable SI from [47] in this setting. Finally, Section V-E details the computational burden associated with SIMBa.⁶

A. Comparing Propositions 1 and 4 using random systems

First, to complement the results in [8] showing the superiority of SIMBa on randomly generated systems when leveraging Proposition 1 to guarantee stability, we use the same simulation setting here to compare the performance when Proposition 4 is used instead. Note that both free parametrizations can capture *all* stable matrices and thus find the true solution (see Corollaries 1 and 3).

To that end, we generated 50 stable discrete-time systems as in [8], with one training, one validation, and one testing trajectory of 300 steps, $n = 5$, $m = 3$, and $r = 3$. The inputs were generated as a Generalised Binary Noise (GBN) input signal with a switching probability of 0.1 for each dimension [11] and white output noise $\mathcal{N}(0, 0.25)$ was added on the training trajectory. For each system, we defined two instances of SIMBa, one with `LMI_A=True` (*SIMBa-1*) and another with `naive_A=True` (*SIMBa-4*), leveraging the corresponding free parametrizations.

First, the performance of each SI method on the testing trajectory from 30 systems is plotted in Fig. 3, where green indicates SIMBa, blue other stable SI methods, and red PARSIM methods, which cannot guarantee stability. For each system, the MSE of every method is normalized with respect to the best-attained performance.

We observe similar performance between both parametrizations, with a slight edge on Proposition 1. It achieved a median

⁵In these cases where $x_0 = 0$, the results found by MATLAB’s SI toolbox [10] turned out to be either comparable or slightly worse than SIPPY’s solutions. They are thus not reported herein. Note that MATLAB’s SI toolbox would outperform SIPPY when $x_0 \neq 0$, as discussed in [8].

⁶The code and data used for these experiments can be found on <https://gitlab.nccr-automation.ch/loris.dinatale/simba>.

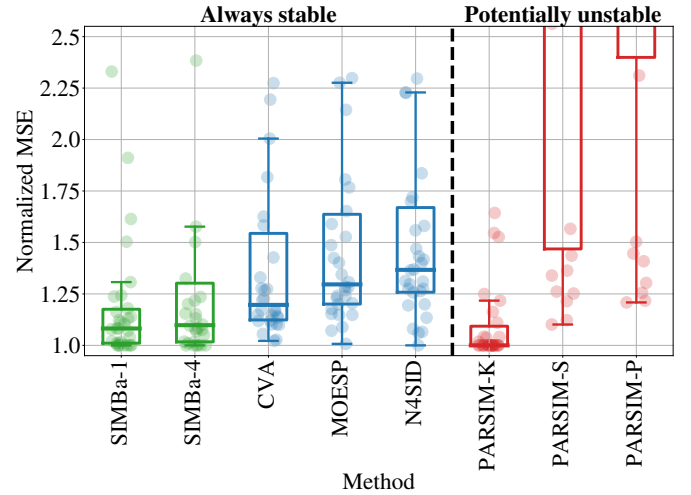


Fig. 3. Performance of input-output state-space identification methods on 30 randomly generated systems, where the MSEs have been normalized by the best-obtained error for each system. The performance of SIMBa (ours) — either relying on the parametrization proposed in Proposition 1 or 4 — is plotted in green, other stable SI methods in blue, and unstable ones in red.

TABLE I
PERFORMANCE DROP OF EACH METHOD COMPARED TO THE BEST ONE, REPORTED FROM FIG. 3.

Method	0.25-quantile	Median	0.75-quantile
SIMBa-1	1.01	1.08	1.18
SIMBa-4	1.02	1.10	1.30
CVA	1.12	1.20	1.54
MOESP	1.20	1.30	1.64
N4SID	1.26	1.37	1.67
PARSIM-K	1.00	1.00	1.09
PARSIM-S	1.47	4.75	30.91
PARSIM-P	2.40	7.00	223.76

performance 8.2% worse than the best method on the different systems, compared to the 9.8% of *SIMBa-4*, as reported in Table I for clarity. Note that PARSIM-K attained impressive performance in this setting — it is the only traditional SI method able to compete with SIMBa in terms of accuracy, confirming the trend observed in [8]. However, it cannot guarantee the stability of the identified model. On the other hand, other stable SI methods reached a performance drop of more than 20% compared to the best method half of the time (see Table I).

Note that *SIMBa-4* additionally shows a slightly less robust performance than *SIMBa-1*, with a wider interquartile range. This hints that while the free parametrization in Proposition 4 does capture all stable matrices, it might be numerically less stable than the LMI-based one from Proposition 1.

Finally, for completeness, we used the other 20 generated systems to assess the impact of data standardization on the final performance. Before the SI procedure, each dimension of the dataset was processed to have zero mean and unit standard deviation, removing the effect of different dimensions having different magnitudes, as is often done in practice. As pictured in Fig. 4, however, little impact can be seen, with the different methods reaching similar performance to what was observed in Fig. 3. On the contrary, there seems to be a

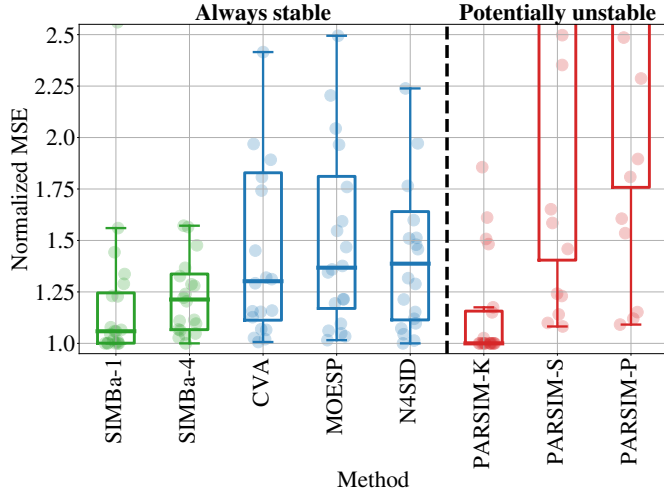


Fig. 4. Performance of input-output state-space identification methods on 20 randomly generated systems, where the data has been standardized and the MSEs have been normalized by the best-obtained error for each system. The performance of SIMBa (ours) — either relying on the parametrization proposed in Proposition 1 or 4 — is plotted in green, other stable SI methods in blue, and potentially unstable ones in red.

slightly wider gap between *SIMBa-1* and the other stable SI approaches in blue. Similarly to the previous case, *SIMBa-4* again slightly underperformed compared to its counterpart leveraging Proposition 1, providing additional indications that the parametrization in Proposition 4 might be numerically more challenging.

Since little performance difference can be observed between Fig. 3 and Fig. 4, data standardization does not seem to impact SIMBa’s performance significantly in general. Interestingly, this means even the gradient-based SIMBa can be run to fit data with different orders of magnitudes accurately. We suspect gradient clipping to be an important reason behind this strong performance, but further analyses would be required to understand the behavior of GD in SIMBa fully.

B. Introducing prior knowledge

As a second case study, we analyzed the effect of incorporating various levels of prior knowledge into SIMBa. To that end, we used the same simulation settings as in Section V-A to create 10 systems but with $n = 7$, $m = 6$, $p = 5$, and trajectories of length 500. Before generating the data, however, we randomly set 60% of the entries of A , B , C , and D to zero.⁷ We used these sparse systems to assess the impact of prior knowledge, i.e., either knowing the sparsity pattern or the true values of one or several of the state-space matrices. We set `LMI_A=True` to leverage Proposition 3 or 1 when `mask_A` is known or not, respectively, and let SIMBa run for 25,000 epochs.

The resulting normalized errors are presented in Fig. 5, where the plot has been generated as in Section V-A, and the bottom figure is a zoomed-in version for better visualization of the differences between the various instances of

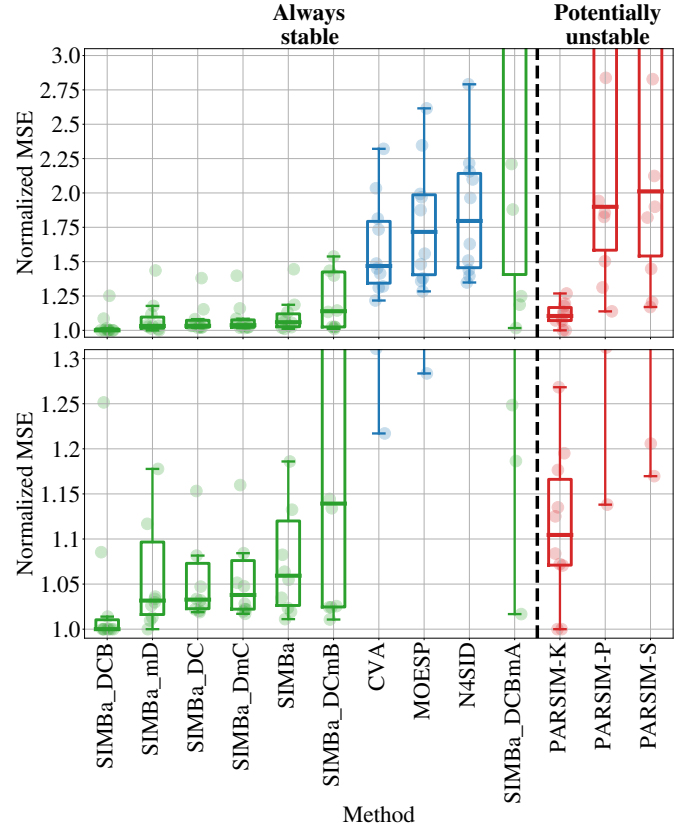


Fig. 5. Normalized MSE of each method on test input-output data from 10 randomly generated systems with sparse matrices A , B , C , and D . The letters after *SIMBa_* encode which matrices X or sparsity pattern mX , respectively, are assumed to be known and fixed. Both plots show the same data with a different zoom to appreciate the difference between SIMBa (ours) and other stable SI methods (in blue) in the top image and show the impact of various levels of prior knowledge on the performance in the bottom one.

SIMBa. The knowledge incorporated in each SIMBa instance is encoded in their name, where “ X ” or “ mX ” indicates that the true matrix X or its true sparsity pattern was given through `{X}_init` or `mask_{X}`, respectively.⁸ For example, *SIMBa_DcMb* represents instances of SIMBa with knowledge of C , D , and the sparsity pattern of B . In practice, this could correspond to a system where $D \equiv 0$ and we know which states are measured (i.e., C is known) and which inputs act on which states but not their exact impact (i.e., the sparsity pattern of B is known). This is encoded in SIMBa by setting `learn_C=learn_D=False`, passing the known matrices C and D as `C_init` and `D_init`, respectively, and defining `mask_B` to be the true known sparsity pattern of B .

Since prior knowledge cannot be enforced in any traditional method, they are only directly comparable with the vanilla system-agnostic *SIMBa*. As expected, similar conclusions as in Section V-A and in [8] can be drawn from the top plot of Fig. 5, with a clear edge of *SIMBa* over other stable SI methods and only PARSIM-K achieving comparable performance. Indeed, traditional stable SI methods lead to relatively poor performance, never coming closer than 20% off the

⁷We made sure that A remained stable after this sparsification procedure.

⁸When the true matrix X is given to SIMBa, `learn_{X}` is set to `False`, so that it is not modified during learning.

best performance and incurring costs over $1.5\text{--}1.75\times$ higher than the best one half of the time. Furthermore, as shown in the bottom plot, PARSIM-K achieved a median gap to the best performance of around 10%, which is worse than most informed SIMBa instances despite not guaranteeing stability.

Interestingly, apart from *SIMBa_DCBmA* — when simultaneously enforcing stability and sparsity of the matrix A with Proposition 3 —, all the informed instances of SIMBa consistently achieve strong performance improvements over traditional stable methods. Most notably, they often outperformed the system-agnostic *SIMBa*, hinting at the efficacy of prior knowledge inclusion in SIMBa. On the one hand, this makes intuitive sense since we pass *true* information to SIMBa, restricting the search space. On the other hand, enforcing fixed matrices or sparsity patterns reduces the expressiveness of the model to fit the training data well — and GD might get stuck in a poor local minimum. Indeed, the set of all possible state-space matrices, over which *SIMBa* optimizes,⁹ contains the sparse matrices the other instances are optimizing over. *SIMBa* might hence find state-space matrices achieving a better MSE without respecting the desired system properties. Although *SIMBa_DCBmA* and, to some extent, *SIMBa_DcMB* seem to have been impacted and stuck in global minima, the other informed versions of SIMBa all perform extremely well.

Altogether, our investigations hint that SIMBa indeed allows one to impose known or desired system properties without sacrificing significant model performance in general. There is however one critical exception: Proposition 3 seems to impose too conservative conditions on sparse matrices, in line with Remark 2, and often led to poor accuracy in this case study (*SIMBa_DCBmA*).

C. Identifying sparse and stable systems

To tackle the aforementioned issue of Proposition 3 being too conservative and constraining the expressiveness of SIMBa, we propose to use Proposition 4 instead in this Section. We used the same settings as in Section V-B to generate 10 new sparse systems and compare the effectiveness of both propositions. In other words, we only considered *SIMBa_DCBmA* here, but using two different free parameterizations of sparse Schur matrices. Furthermore, to ensure randomness did not have a significant impact on the results, we let SIMBa run with seven different random seeds in each case. All the results are plotted in Fig. 6. To better assess the potential of SIMBa, Fig. 7 displays the results when only considering the best-performing seed on each system, and the corresponding key metrics are reported in Table II for clarity.

As expected from what could be observed in Fig. 5, *SIMBa-3* performed very poorly in general, even if it was run several times. Interestingly, this analysis hints that the effectiveness of Proposition 3 depends more on system-intrinsic characteristics than on the random seed used. Indeed, although not fully visible in the plots of Fig. 6 and 7, the performance distribution of *SIMBa-3* shows similar statistics whether all the results or only the best seeds are considered. This eliminates

⁹More specifically, it optimizes over the space of stable matrices A and generic matrices B , C , and D .

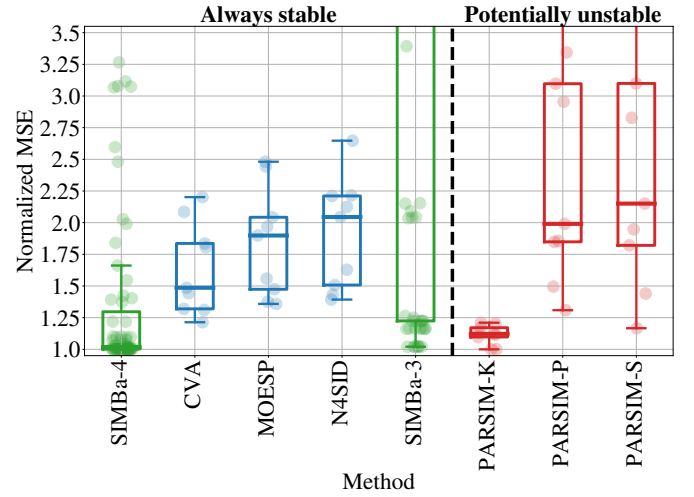


Fig. 6. Performance of each method, normalized by the best one, on test input-output data from 10 randomly generated systems with sparse matrices A , B , C , and D . The performance of SIMBa (ours) — either relying on Proposition 3 or 4 — is plotted in green, other stable SI methods in blue, while red indicates methods without stability guarantees. Note that SIMBa was run with 7 different random seeds on each system.

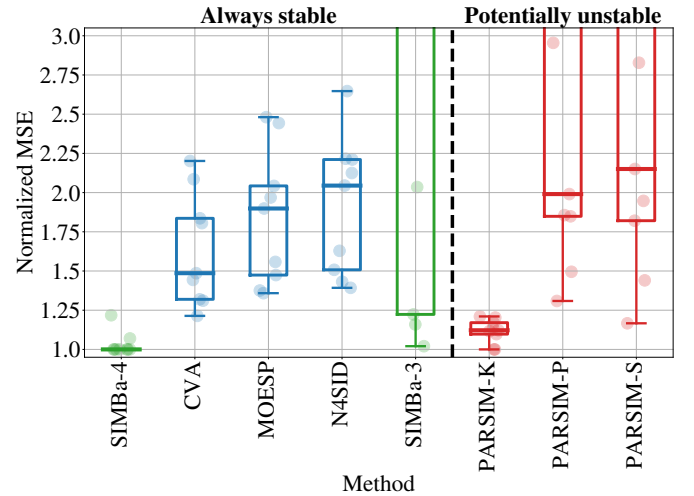


Fig. 7. Performance of each method, normalized by the best one, on test input-output data from 10 randomly generated systems with sparse matrices A , B , C , and D . The performance of SIMBa (ours) — either relying on the parametrization proposed in Proposition 3 or 4 — is plotted in green, other stable SI methods in blue, while red indicates methods without stability guarantees. Note that SIMBa was run with 7 different random seeds on each system and we report here the best-obtained performance in each case.

the effect of randomness to some extent and supports the hypothesis that the parametrization in (11) is too conservative (see Remark 2).

On the other hand, *SIMBa-4* achieved excellent performance in general, as shown in Fig. 6, outperforming every other stable SI method, with PARSIM-K being the only one attaining similar accuracy. In fact, 75% of its instances achieved a performance gap below 30% while all the other stable SI methods in blue had a gap worse than that more than 75% of the time. However, it seems to be more sensitive to randomness,

TABLE II
PERFORMANCE DROP OF EACH METHOD COMPARED TO THE BEST ONE,
CORRESPONDING TO FIG. 7.

Method	0.25-quantile	Median	0.75-quantile
SIMBa-4	1.00	1.00	1.00
CVA	1.32	1.49	1.84
MOESP	1.47	1.90	2.04
N4SID	1.51	2.04	2.21
SIMBa-3	1.22	5.18	11.43
PARSIM-K	1.10	1.12	1.17
PARSIM-P	1.85	1.99	3.10
PARSIM-S	1.82	2.15	3.10

with some instances achieving relatively poor performance, especially compared to the very consistent results obtained by PARSIM-K. Interestingly, this does not seem to be system-dependent, and *SIMBa-4* could achieve very good performance on all the systems, as plotted in Fig. 7.

Although running several instances of SIMBa naturally incurs additional computational cost, Fig. 7 hints that it can be beneficial to find a better-performing model. If only the best seed is considered, SIMBa might even consistently outperform PARSIM-K. In this case study, *SIMBa-4* could simultaneously beat all other stable methods by more than 25% on all systems. Collectively, these results show that introducing prior knowledge on the sparsity of A does not necessarily come at the price of performance, complementing what was observed in Section V-B for other knowledge integration schemes.

D. Performance on real-world input-state data

To showcase SIMBa's versatility, we now turn to an input-state data set collected from the Franka Emika Panda robotic arm and provided in [47]. We have access to eight trajectories of length $N = 400$, samples at 50 Hz, with $n = 17$ and $m = 7$. We fixed one validation and one test trajectory, respectively, and used a subset of the remaining six trajectories as training data. Since the robot is a continuous-time system, we leveraged Proposition 2, setting $\delta = \frac{1}{50}$ and $\text{LMI_A} = \text{True}$. As we are not dealing with input-output data anymore, subspace identification methods perform poorly, and we hence compare SIMBa to LS and its state-of-the-art stable version, SOC, proposed in [47].

Here, we also used the ability of SIMBa to work with batched data, breaking the training trajectories into 10-step long segments, overlapping at each time step, — i.e., setting $\text{horizon}=10$ and $\text{stride}=1$ — to facilitate training for this more complex problem. This gave rise to approximately 400 to 2,400 training sequences of 10 steps whether one to six trajectories were used for training. Since we are interested in the final performance of SIMBa over entire trajectories, we set $\text{horizon_val}=\text{None}$ to select the best model accordingly. We let instances initialized with the LS solution (*SIMBa_i*) and randomly initialized ones (*SIMBa*) run for 20,000 and 40,000 epochs, respectively, with a batch size of 128.

The MSE of each method on the test trajectory is reported in Fig. 8 with a logarithmic scale, where the x-axis enumerates which trajectories were used for training. Similarly to the previous Section, SIMBa was run 10 times in each case to assess the impact of randomness. As expected, we see a general

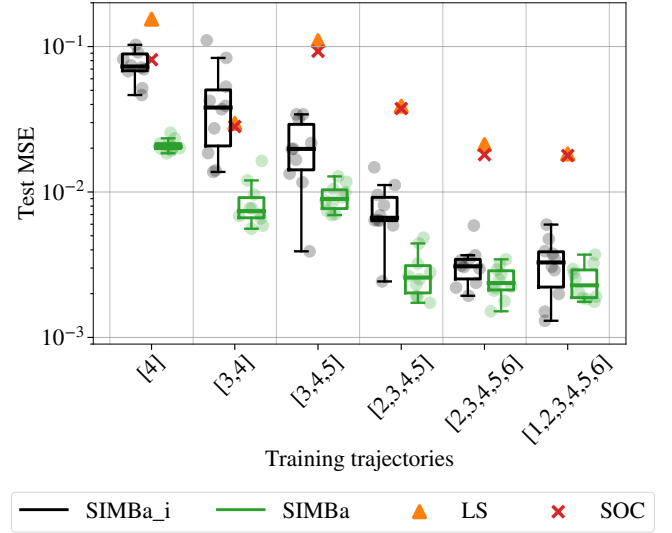


Fig. 8. MSE of each method on the test trajectory of the Franka data set after training from different trajectories. Black and green data show the performance of SIMBa over 10 runs with informed (*SIMBa_i*) and random initialization (*SIMBa*), respectively. The MSE of LS and SOC are reported in orange triangles and red crosses, respectively.

tendency of all the methods to find more accurate solutions with more training data. Interestingly, *SIMBa* often performs better than *SIMBa_i* on this data, hinting that initializing SIMBa with the matrices found through LS might stick it in relatively poor local minima.

Overall, SIMBa generally outperformed LS and SOC, and often significantly, especially when more training data was available. The only exceptions came from *SIMBa_i* when one or two trajectories only were used for training, where we can see performance drops for some instances. On the other hand, *SIMBa* always outperformed LS and SOC, and with an impressive median performance improvement compared to SOC of over 70% and as high as 95%, as reported in Fig. 9. Here, the *improvement* is computed as

$$\text{Improvement} = 100 \left(1 - \frac{\text{MSE}_{\text{SIMBa}}}{\text{MSE}_{\text{SOC}}} \right).$$

Moreover, looking at the best-achieved performance of *SIMBa* and *SIMBa_i*, they attained improvements of over 90% compared to SOC as soon as more than three training trajectories were used. When only one or two trajectories were leveraged for training, *SIMBa_i* achieved 42% or 51% better performance than SOC, respectively, and this improvement increases to 77% or 80% for *SIMBa*.

In general, we suspect the observed performance gaps to be heavily impacted by the ability of SIMBa to minimize the error over *multiple steps*, here ten, compared to myopic classical LS-based methods. This showcases the usefulness of backpropagation-based approaches, which can handle complex fitting criteria instead of the classical one-step-ahead prediction error.

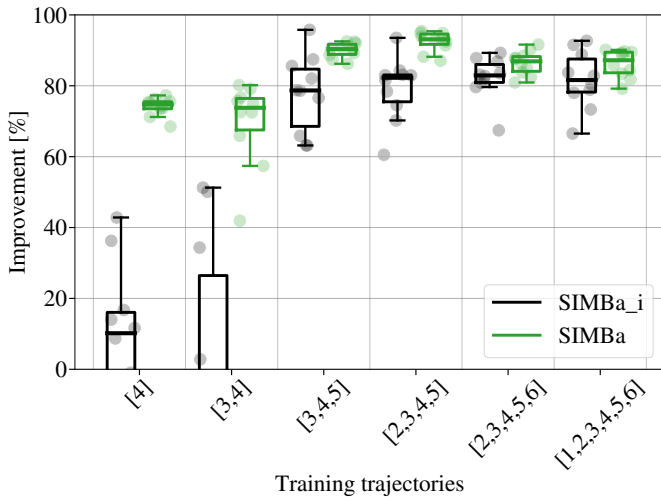


Fig. 9. Improvement of SIMBa over SOC on the test data from the Franka robotic arm for different training trajectories, reported from Fig. 8.

TABLE III
AVERAGE RUNNING TIME IN SECONDS OF EACH METHOD IN SECTION V-B.

Method	Time	Method	Time
N4SID	0.25	SIMBa	3718
MOESP	0.31	SIMBa_mD	3697
CVA	0.56	SIMBa_mC	3497
		SIMBa_C	3373
PARSIM-K	1.47	SIMBa_CmB	3660
PARSIM-S	1.11	SIMBa_CB	3112
PARSIM-P	7.87	SIMBa_CBmA	3089

E. Training complexity

To conclude these numerical investigations, this Section provides insights into the training time of different versions of SIMBa. All the experiments were run on a Bizon ZX5000 G2 workstation. Note that while a Graphical Processing Unit (GPU) interface is implemented, we did not use it to obtain the results presented in this paper, setting `device='cpu'`. Indeed, using GPUs for such small-scale problems generally slows the overall training time since the overhead required to move data and models to the GPU at each iteration is higher than the subsequent optimization time gain.

First, as reported in Table III, each instance of SIMBa ran for slightly less than 1 h in Section V-B, which is several orders of magnitude slower than the few seconds required to fit traditional SI methods. Interestingly, however, enforcing prior knowledge did not significantly impact its run-time. Since fewer parameters need to be learned from data, informed versions tended to take less time per epoch. This stems from SIMBa's architecture and unconstrained training procedure in (13) or (16). It allows SIMBa to seamlessly guarantee the desired system properties through modifications of (14)–(15) — for example, to (19) — without additional computational burden.

Note that these SIMBa instances were run for 25,000 epochs, and doubling that number would hence double their training time to approximately 2 h. The training procedure would then be comparable to *SIMBa_L* in [8], which was

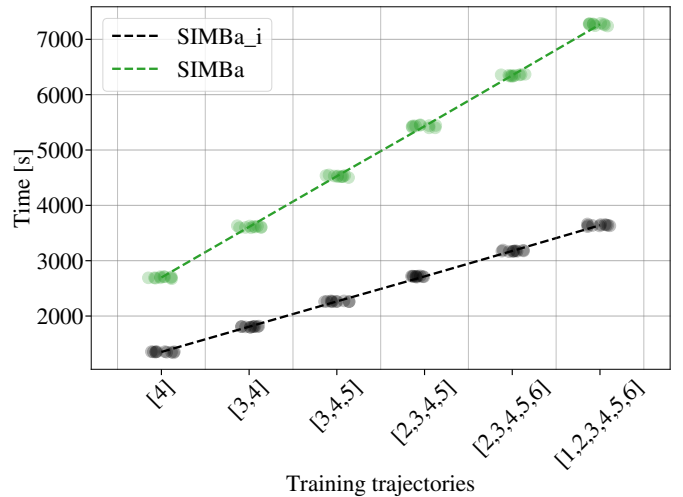


Fig. 10. Running time for SIMBa (in seconds), reported from Fig. 8. Note that this does not include approximately 130 s required to initialize *SIMBa_i* for 150,000 epochs.

reported to take roughly 25 min for 50,000 epochs, i.e., around five times less. However, the latter was trained over 100 data points, compared to 500 in Section V-B, revealing an approximately linear relationship between the horizon length and training complexity.

For completeness, the training times of the SIMBa instances analyzed in Section V-D are shown in Fig. 10, exposing the expected linear impact of leveraging more and more training data. However, five to six times more data can be used before doubling the training time, leveled by `PyTorch`'s capability to process several trajectories in parallel. Unsurprisingly, on the other hand, doubling the number of iterations approximately yields twice longer fitting times (comparing *SIMBa_i* to *SIMBa*).

As a final remark, we would like to highlight here that all the analyzed instances of SIMBa were usually run for more epochs than required to ensure convergence. In practice, one could interrupt the training once the validation error stagnates or augments, showing SIMBa started to overfit the training data. To illustrate this, Fig. 11 reports the time required by SIMBa to achieve its best performance on the validation data set — these state-space matrices are the ones ultimately employed to assess its performance on the testing data. As can be seen, SIMBa sometimes identifies the best-performing solution in considerably less time than the total allowed training time. Similarly, the learning rate could be increased in practice to converge faster to these solutions; however, a comprehensive analysis of its influence was out of the scope of this manuscript.

VI. DISCUSSION

With the investigations in the previous Section showcasing SIMBa's performance on various system identification tasks, let us now briefly summarise how to best use the toolbox to maximize its performance and discuss potentially interesting extensions to it.

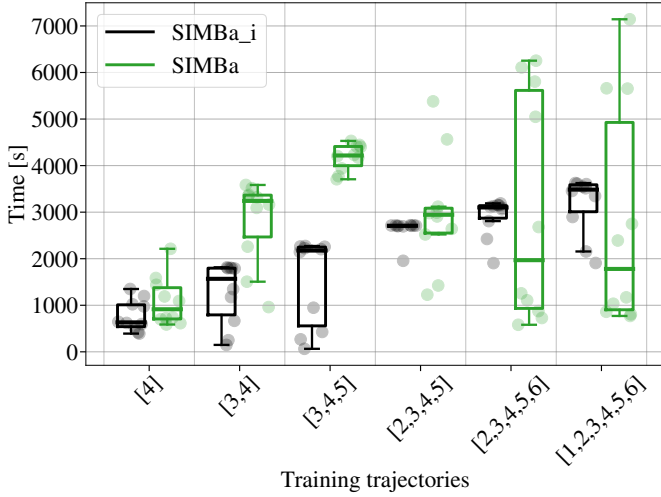


Fig. 11. Time required for SIMBa to achieve its best validation error (in seconds), to compare with the corresponding total training times shown in Fig. 10.

A. A summary of SIMBa's capabilities

While SIMBa can achieve significant performance gains over traditional methods in many different settings, the associated computational burden can be significant. Indeed, even simple systems take several minutes to be fit, and this can grow significantly with longer training trajectories or when more epochs are required, as detailed in Section V-E. Despite its ability to leverage out-of-the-box ML tools and GPUs, SIMBa is hence not well-suited for problems that demand fast solutions. In practice, traditional methods, which can be trained in a matter of seconds, are thus generally a good starting point. On the other hand, for cases where achieving the best performance is critical or when desired system properties need to be preserved, SIMBa can be extremely beneficial, as presented in Section V.

During our investigations, we saw that randomness could play a significant role; running several instances of SIMBa might greatly improve its performance. Although initializing its state matrices with the one found by classical methods usually accelerates convergence, we also observed cases where randomly initialized versions achieve better final performance. Both options should hence be considered in practice.

The free parameterizations from Propositions 1–4 can be leveraged to guarantee the stability of the identified model. While Proposition 4 can characterize any Schur matrix, it seems to be more sensitive to randomness and more numerically challenging than the other parametrizations. In practice, Propositions 1 and 2 should thus be preferred, and only the too-conservative Proposition 3 should be discarded in favor of Proposition 4.

In general, the provided default parameters perform well — they have indeed demonstrated robust performance across the variety of case studies analyzed in Section V. To maximize the effectiveness of SIMBa, one might consider increasing the number of training epochs, for instance. On the other hand, the learning rate of 0.001 chosen in this work is sometimes

slower than required. This default option proved to be robust across various tasks, but it might be possible to accelerate learning by taking larger parameter updates at each step on some problems.

B. Potential extensions

Throughout Section V, we did not strain to obtain the best performance on each case study but focused on fair comparisons between different methods under identical conditions. In practical applications, one should combine SIMBa — or any SI method — with data processing procedures, such as standardization, detrending, or filtering, to improve performance. In general, an interface with MATLAB's SI toolbox, which comes with many useful helper functions, would be an interesting extension to SIMBa.

Apart from better integration of such existing tools, to facilitate training on nonconvex long-horizon objectives, *curriculum learning* could be adopted. In this framework, the training starts with the minimization of the one-step-ahead prediction error and then gradually increases the prediction horizon toward the desired one [48]. This could help SIMBa in the early stage of training, accelerating the first iterations by simplifying the problem — similar in spirit to the proposed initialization from the solution of classical SI methods — before leveraging the full power of automatic backpropagation for long-horizon optimization.

Interestingly, Proposition 4 could also be used to generate affinely parametrized Schur matrices, similar to those examined in [49], for example. The generality of this free parametrization could thus allow SIMBa to guarantee stability while enforcing desired properties on A beyond specific sparsity patterns.

In parallel with these efforts to enforce additional system properties, including nonlinearities may be crucial for some applications. Indeed, linear models might not be flexible enough to fit more complex systems. Thanks to the AD backbone used by SIMBa, NNs can be seamlessly added on top of the linear model, learning patterns that are not well-captured by the linear part, such as in [37]. Otherwise, inspired by the SINDy toolbox [50], if the class of nonlinearities impacting the dynamics are known, one could extend the state description to $f(x) \in \mathbb{R}^{n'}$, for example, including polynomials like $f(x) = [x^\top, (x^2)^\top]^\top$, and then fit a linear model of the form $x_{k+1} = Af(x_k) + Bu(k)$. Finally, a more cumbersome approach would be to discard the linear framework altogether, write custom dynamics, and then leverage automatic backpropagation as proposed herein to find the required parameters, similar to what was proposed in [36] for irreversible port-Hamiltonian systems.

To conclude this discussion, we want to point out a potential link to Koopman-based approaches like [38], where traditional SI methods were used to identify linear models in the corresponding lifted space. Thanks to SIMBa's construction relying on unconstrained GD, the lifting functions could also be learned simultaneously with the lifted linear model, similar in spirit to [39]–[41], potentially improving the accuracy of the end-to-end pipeline without jeopardizing stability.

VII. CONCLUSION

In this paper, we extended the SIMBa toolbox to allow for prior system knowledge integration into the identified state-space matrices, going beyond standard stability conditions. Leveraging novel free parametrizations of Schur matrices to ensure the stability of the identified model despite enforcing desired properties, such as sparsity, we showed how SIMBa outperforms traditional SI methods, and often by more than 25%. Notably, this performance gap grew to 50% when SIMBa had access to prior knowledge about the system, which cannot be enforced by traditional input-output system identification methods. Furthermore, on a real-world robot data set, SIMBa often improved state-of-the-art input-state identification methods by more than 70%, with the gap widening as more and more training data became available.

On the other hand, the significant and consistent performance gains observed across the different numerical experiments proposed in this work come with a large computational burden. SIMBa indeed incurred training times ranging from several minutes to two hours in the various case studies. While this might be alleviated in practice by reducing the number of training epochs, augmenting the step size, or initializing SIMBa with matrices known to perform well, it is important to note that the latter does not necessarily improve the final performance.

In the future, it would be interesting to analyze the theoretical implications of SIMBa and explore potential connections to traditional system identification methods. In another line of work, SIMBa's potential to be incorporated in Koopman-based approaches with stability guarantees is worth investigating. Leveraging the seamless capacity of PyTorch to incorporate various differentiable nonlinear functions, SIMBa has the potential to serve as the foundation for a general tool for knowledge-grounded structured nonlinear system identification.

APPENDIX

A. Proof of Corollary 1

Let A be a Schur matrix and $\epsilon > 0$. Setting $\gamma = 1$ in [51, Theorem 2.2], we know there exists a symmetric Lyapunov function $Q = Q^\top \succ 0$ with

$$\begin{bmatrix} Q & AQ \\ Q^\top A^\top & Q \end{bmatrix} \succ 0 \iff Q - AQA^\top \succ 0,$$

where the equivalence follows from Schur's complement. Introducing a free parameter $G \in \mathbb{R}^{n \times n}$ and the transformation $T = [I, -A]$, this can be rewritten as

$$\begin{aligned} & Q - AGA^\top - A^\top G^\top A \\ & \quad + AGA^\top + A^\top G^\top A - AQA^\top \succ 0 \\ \iff & T \begin{bmatrix} Q & AG \\ G^\top A^\top & G^\top + G - Q \end{bmatrix} T^\top \succ 0 \\ \iff & \begin{bmatrix} Q & AG \\ G^\top A^\top & G^\top + G - Q \end{bmatrix} =: \Gamma \succ 0. \end{aligned} \quad (20)$$

In words, if A is Schur stable, there exists $Q \succ 0$ and G such that (20) holds. Then, for any $\alpha > 0$, αQ and αG are valid

alternative choices of Lyapunov function and free parameter because $\alpha Q = \alpha Q^\top \succ 0$ and

$$\begin{bmatrix} \alpha Q & A(\alpha G) \\ \alpha G^\top A^\top & \alpha G^\top + \alpha G - \alpha Q \end{bmatrix} = \alpha \Gamma \succ 0.$$

Since Γ is positive definite, $\lambda_{\min}(\Gamma) > 0$, and we can set

$$\alpha := \frac{2\epsilon}{\lambda_{\min}(\Gamma)} > 0, \quad \Delta := \alpha \Gamma - \epsilon \mathbb{I}_{2n}.$$

Then, according to Weyl's inequality [52], we have

$$\begin{aligned} \lambda_{\min}(\Delta) & \geq \lambda_{\min}(\alpha \Gamma) - \lambda_{\max}(\epsilon \mathbb{I}_{2n}) \\ & = \alpha \lambda_{\min}(\Gamma) - \epsilon = 2\epsilon - \epsilon = \epsilon > 0, \end{aligned}$$

so that $\Delta = \Delta^\top \succ 0$. We can then define $W = \Delta^{\frac{1}{2}}$, set $V = 0$ and construct A as in (4), with S as in (3). \square

B. Proof of Proposition 2

We need to show that A as defined in (4) is Schur, i.e., the autonomous system

$$x_{k+1} = Ax_k \quad (21)$$

is stable. This is equivalent to finding a matrix $Q = Q^\top \succ 0$ that solves the following Lyapunov inequality [43]:

$$Q - A^\top QA \succ 0. \quad (22)$$

By definition of A , we have

$$\begin{aligned} & Q - A^\top QA \succ 0 \\ \iff & Q - (I_n + \delta \bar{A})^\top Q (I_n + \delta \bar{A}) \succ 0 \\ \iff & Q - Q - \delta Q \bar{A} - \delta \bar{A}^\top Q - \delta^2 \bar{A}^\top Q \bar{A} \succ 0 \\ \iff & -\delta Q \bar{A} - \delta \bar{A}^\top Q - \delta^2 \bar{A}^\top Q \bar{A} \succ 0. \end{aligned}$$

Let us decompose \bar{A} as $\bar{A} = E^{-1}F$ for suitable matrices E and F . We can then rewrite the last inequality as

$$-\delta QE^{-1}F - \delta F^\top E^{-\top}Q - \delta^2 F^\top E^{-\top}QE^{-1}F \succ 0.$$

Defining $P = E^{-\top}QE^{-1} \succ 0$ and dividing by δ , this can be rewritten as

$$-QE^{-1}F - F^\top E^{-\top}Q - \delta F^\top PF \succ 0. \quad (23)$$

Since $Q = E^\top PE$, (23) is equivalent to

$$-E^\top PF - F^\top PE - \delta F^\top PF \succ 0.$$

Using Schur's complement, this can be rewritten as

$$\begin{bmatrix} -E^\top PF - F^\top PE & F^\top \\ F & \frac{1}{\delta} P^{-1} \end{bmatrix} \succ 0. \quad (24)$$

In words, A as in (8) is Schur if and only if there exist $P \succ 0$, E , and F such that $\bar{A} = E^{-1}F$ and (20) holds.

Let us now parametrize the left-hand side of the above LMI with S from (7). Critically, (24) will always be satisfied since S is positive definite by construction for any choice of W , ensuring the stability of A . Since $S_{22} = S_{22}^\top$, we can then recover

$$P = \frac{S_{22}^{-1}}{\delta}, \quad F = S_{21} = S_{12}^\top.$$

Knowing that $S_{11}^\top = S_{11}$ by definition and that

$$-E^\top PF - F^\top PE = S_{11}$$

needs to hold, we can set

$$\begin{aligned} F^\top PE &= -\frac{S_{11}}{2} + V - V^\top \\ \implies E^{-1} &= -2(S_{11} + V - V^\top)^{-1} F^\top P, \end{aligned}$$

for any $V \in \mathbb{R}^{n \times n}$. Since $\bar{A} = E^{-1}F$, this leads to

$$\begin{aligned} \bar{A} &= -2(S_{11} + V - V^\top)^{-1} F^\top PF \\ &= -\frac{2}{\delta}(S_{11} + V - V^\top)^{-1} S_{12} S_{22}^{-1} S_{21} \end{aligned}$$

and

$$A = I + \delta \bar{A} = I - 2(S_{11} + V - V^\top)^{-1} S_{12} S_{22}^{-1} S_{21}. \square$$

C. Proof of Corollary 2

Let A be a Schur matrix and $\epsilon > 0$. Setting $E = \mathbb{I}_n$ and $F = \bar{A}$ in the proof of Proposition 2, there exists a Lyapunov function $P = P^\top \succ 0$ such that (24) holds. Similarly to the proof of Corollary 1, for any $\alpha > 0$, αE , αF , and $\frac{P}{\alpha}$ are valid alternative choices since

$$\begin{bmatrix} -\alpha E^\top \frac{P}{\alpha} \alpha F - \alpha F^\top \frac{P}{\alpha} \alpha E & \alpha F^\top \\ \alpha F & \frac{1}{\delta} \alpha P^{-1} \end{bmatrix} \succ 0$$

and $(\alpha E)^{-1} \alpha F = \bar{A}$. One can then set $V = 0$ and follow the proof of Corollary 1 to find suitable values for α and W such that (8) holds for S as in (7). \square

D. Proof of Proposition 3

1) *Preliminaries:* Throughout the proof below, we will use the following properties of the Hadamard product, for any matrices $K, L, M \in \mathbb{R}^{n \times n}$ and diagonal matrix $\Lambda \in \mathbb{R}^{n \times n}$ [52]:

$$(P1) \quad (K \odot L) + (K \odot M) = K \odot (L + M),$$

$$(P2) \quad (L \odot M)^\top = (L^\top \odot M^\top),$$

$$(P3) \quad (K \odot L)(\Lambda \odot M) = K \odot (L(\Lambda \odot M)),$$

where the last property holds since Λ is diagonal.

2) *Proof of Proposition 3:* As in the proof of Proposition 2, we need to find a symmetric matrix $Q = Q^\top \succ 0$ such that $Q - A^\top Q A \succ 0$. Following the proof of Corollary 1, one can show that this is equivalent to finding $Q = Q^\top \succ 0$ such that

$$\begin{bmatrix} Q & AG \\ G^\top A^\top & G^\top + G - Q \end{bmatrix} \succ 0, \quad (25)$$

where $G \in \mathbb{R}^{n \times n}$ is a free parameter. In this sparse case, we consider diagonal Q and G matrices of the form

$$Q = N \odot P, \quad G = N \odot H,$$

for some $P, H \in \mathbb{R}^{n \times n}$ and with N defined in (10). Note here that this also implies $Q = Q^\top$, as required in (25). Recalling that we want to identify a matrix A of the form $A = \mathcal{M} \odot \bar{A}$ for some \bar{A} , (25) can be written as

$$\begin{aligned} &\begin{bmatrix} N \odot P & (\mathcal{M} \odot \bar{A})(N \odot H) \\ (*)^\top & (N \odot H)^\top + (N \odot H) - (N \odot P) \end{bmatrix} \succ 0 \\ &\stackrel{(P1)}{\iff} \begin{bmatrix} N \odot P & (\mathcal{M} \odot \bar{A})(N \odot H) \\ (*)^\top & N \odot (H^\top + H - P) \end{bmatrix} \succ 0, \end{aligned}$$

where $(*)^\top$ represents the transpose of the upper right block. Since N is a diagonal matrix, using (P3), we can rewrite the above LMI as

$$\begin{aligned} &\begin{bmatrix} N \odot P & \mathcal{M} \odot (\tilde{A}(N \odot H)) \\ ((\mathcal{M} \odot (\tilde{A}(N \odot H)))^\top & N \odot (H^\top + H - P) \end{bmatrix} \succ 0 \\ &\stackrel{(P2)}{\iff} \begin{bmatrix} N \odot P & \mathcal{M} \odot (\tilde{A}(N \odot H)) \\ \mathcal{M}^\top \odot (\tilde{A}(N \odot H))^\top & N \odot (H^\top + H - P) \end{bmatrix} \succ 0 \\ &\iff \begin{bmatrix} N & \mathcal{M} \\ (*)^\top & N \end{bmatrix} \odot \begin{bmatrix} P & \tilde{A}(N \odot H) \\ (*)^\top & H^\top + H - P \end{bmatrix} \succ 0. \end{aligned} \quad (26)$$

A sufficient condition for the above Hadamard product to be positive semi-definite is to ensure that both factors are individually positive semi-definite [53], i.e.,

$$\begin{bmatrix} N & \mathcal{M} \\ (*)^\top & N \end{bmatrix} \succ 0 \quad (27)$$

$$\begin{bmatrix} P & \tilde{A}(N \odot H) \\ (*)^\top & H^\top + H - P \end{bmatrix} \succ 0. \quad (28)$$

Since \mathcal{M} is fixed and known, (27) is satisfied by construction of N in (10) according to the Levy-Desplanques theorem [52]. To satisfy (28), as in Proposition 2, we parametrize its left-hand side with S in (9), which allows us to recover

$$P = S_{11}, \quad H + H^\top = S_{22} + P.$$

As before, by symmetry of S_{11} and S_{22} , for any V , the right equation is satisfied for

$$H = \frac{1}{2}(S_{11} + S_{22}) + V - V^\top.$$

Finally,

$$\begin{aligned} \tilde{A} &= S_{12}(N \odot H)^{-1} \\ &= S_{12} \left[N \odot \left(\frac{1}{2}(S_{11} + S_{22}) + V - V^\top \right) \right]^{-1} \end{aligned}$$

and

$$\begin{aligned} A &= \mathcal{M} \odot \tilde{A} \\ &= \mathcal{M} \odot \left(S_{12} \left[N \odot \left(\frac{1}{2}(S_{11} + S_{22}) + V - V^\top \right) \right]^{-1} \right). \square \end{aligned}$$

E. Proof of Proposition 4

First, the desired sparsity pattern is achieved because

$$\frac{\sigma(\eta)\gamma}{|\lambda(\mathcal{M} \odot V)|_{\max}} (\mathcal{M} \odot V) = \mathcal{M} \odot \left(\frac{\sigma(\eta)\gamma}{|\lambda(\mathcal{M} \odot V)|_{\max}} V \right)$$

by definition of the Hadamard product since the maximum eigenvalue is a scalar.

To show that A is Schur with eigenvalues in a circle of radius γ centered at the origin, suppose β is an eigenvalue of $(\mathcal{M} \odot V)$ corresponding to the eigenvector e , i.e., $(\mathcal{M} \odot V)e = \beta e$. Then,

$$\begin{aligned} Ae &= \frac{\sigma(\eta)\gamma}{|\lambda(\mathcal{M} \odot V)|_{\max}} (\mathcal{M} \odot V) e \\ &= \frac{\sigma(\eta)\gamma}{|\lambda(\mathcal{M} \odot V)|_{\max}} \beta e =: \alpha e, \end{aligned}$$

so that e is still an eigenvector of A , with eigenvalue α . By definition of $|\lambda(\mathcal{M} \odot V)|_{\max}$ and since $0 < \sigma(\eta) < 1$, we obtain

$$|\alpha| = \frac{\sigma(\eta)\gamma}{|\lambda(\mathcal{M} \odot V)|_{\max}} |\beta| < \frac{|\beta|}{|\lambda(\mathcal{M} \odot V)|_{\max}} \gamma \leq \gamma,$$

hence, concluding the proof. \square

REFERENCES

- [1] Y. Goldberg, *Neural network methods for natural language processing*. Springer Nature, 2022.
- [2] W. Rawat and Z. Wang, “Deep convolutional neural networks for image classification: A comprehensive review,” *Neural computation*, vol. 29, no. 9, pp. 2352–2449, 2017.
- [3] L. Ljung, C. Andersson, K. Tiels, and T. B. Schön, “Deep learning and system identification,” *IFAC-PapersOnLine*, vol. 53, no. 2, pp. 1175–1181, 2020.
- [4] M. Forgione and D. Piga, “Continuous-time system identification with neural networks: Model structures and fitting criteria,” *European Journal of Control*, vol. 59, pp. 69–81, 2021.
- [5] S. L. Brunton and J. N. Kutz, *Data-driven science and engineering: Machine learning, dynamical systems, and control*. Cambridge University Press, 2022.
- [6] L. Ljung, “System identification,” in *Signal analysis and prediction*. Springer, 1998, pp. 163–173.
- [7] D. Gedon, N. Wahlström, T. B. Schön, and L. Ljung, “Deep state space models for nonlinear system identification,” *IFAC-PapersOnLine*, vol. 54, no. 7, pp. 481–486, 2021.
- [8] L. Di Natale, M. Zakwan, B. Svetozarevic, P. Heer, G. F. Trecate, and C. N. Jones, “Stable Linear Subspace Identification: A Machine Learning Approach,” *arXiv preprint arXiv:2311.03197*, 2023.
- [9] A. Paszke, S. Gross, F. Massa, A. Lerer, J. Bradbury, G. Chanan, T. Killeen, Z. Lin, N. Gimelshein, L. Antiga, A. Desmaison, A. Kopf, E. Yang, Z. DeVito, M. Raison, A. Tejani, S. Chilamkurthy, B. Steiner, L. Fang, J. Bai, and S. Chintala, “Pytorch: An imperative style, high-performance deep learning library,” in *Advances in Neural Information Processing Systems* 32. Curran Associates, Inc., 2019, pp. 8024–8035. [Online]. Available: <http://papers.neurips.cc/paper/9015-pytorch-an-imperative-style-high-performance-deep-learning-library.pdf>
- [10] L. Ljung, *System identification toolbox: User's guide*. Citeseer, 1995.
- [11] G. Armenise, M. Vaccari, R. B. Di Capaci, and G. Pannocchia, “An open-source system identification package for multivariable processes,” in *2018 UKACC 12th International Conference on Control (CONTROL)*. IEEE, 2018, pp. 152–157.
- [12] S. J. Qin, “An overview of subspace identification,” *Computers & chemical engineering*, vol. 30, no. 10–12, pp. 1502–1513, 2006.
- [13] P. Van Overschee and B. De Moor, “N4SID: Subspace algorithms for the identification of combined deterministic-stochastic systems,” *Automatica*, vol. 30, no. 1, pp. 75–93, 1994.
- [14] M. Verhaegen and P. Dewilde, “Subspace model identification part 2. Analysis of the elementary output-error state-space model identification algorithm,” *International journal of control*, vol. 56, no. 5, pp. 1211–1241, 1992.
- [15] W. E. Larimore, “Canonical variate analysis in identification, filtering, and adaptive control,” in *29th IEEE Conference on Decision and control*. IEEE, 1990, pp. 596–604.
- [16] P. Van Overschee and B. De Moor, “A unifying theorem for three subspace system identification algorithms,” *Automatica*, vol. 31, no. 12, pp. 1853–1864, 1995.
- [17] S. J. Qin, W. Lin, and L. Ljung, “A novel subspace identification approach with enforced causal models,” *Automatica*, vol. 41, no. 12, pp. 2043–2053, 2005.
- [18] S. J. Qin and L. Ljung, “Parallel QR implementation of subspace identification with parsimonious models,” *IFAC Proceedings Volumes*, vol. 36, no. 16, pp. 1591–1596, 2003.
- [19] G. Pannocchia and M. Calosi, “A predictor form PARSIMonious algorithm for closed-loop subspace identification,” *Journal of Process Control*, vol. 20, no. 4, pp. 517–524, 2010.
- [20] J. M. Maciejowski, “Guaranteed stability with subspace methods,” *Systems & Control Letters*, vol. 26, no. 2, pp. 153–156, 1995.
- [21] B. Boots, G. J. Gordon, and S. Siddiqi, “A constraint generation approach to learning stable linear dynamical systems,” *Advances in neural information processing systems*, vol. 20, 2007.
- [22] S. L. Lacy and D. S. Bernstein, “Subspace identification with guaranteed stability using constrained optimization,” *IEEE Transactions on automatic control*, vol. 48, no. 7, pp. 1259–1263, 2003.
- [23] N. Gillis, M. Karow, and P. Sharma, “A note on approximating the nearest stable discrete-time descriptor systems with fixed rank,” *Applied Numerical Mathematics*, vol. 148, pp. 131–139, 2020.
- [24] W. Jongeneel, T. Sutter, and D. Kuhn, “Efficient learning of a linear dynamical system with stability guarantees,” *IEEE Transactions on Automatic Control*, 2022.
- [25] G. Mamakoukas, I. Abraham, and T. D. Murphey, “Learning stable models for prediction and control,” *IEEE Transactions on Robotics*, 2023.
- [26] A. Haber and M. Verhaegen, “Subspace identification of large-scale interconnected systems,” *IEEE Transactions on Automatic Control*, vol. 59, no. 10, pp. 2754–2759, 2014.
- [27] P. Massioni and M. Verhaegen, “Subspace identification of circulant systems,” *Automatica*, vol. 44, no. 11, pp. 2825–2833, 2008.
- [28] —, “Subspace identification of distributed, decomposable systems,” in *Proceedings of the 48th IEEE Conference on Decision and Control (CDC) held jointly with 2009 28th Chinese Control Conference*. IEEE, 2009, pp. 3364–3369.
- [29] C. Yu and M. Verhaegen, “Subspace identification of distributed clusters of homogeneous systems,” *IEEE Transactions on Automatic Control*, vol. 62, no. 1, pp. 463–468, 2016.
- [30] Y. Li, Z. O’Neill, L. Zhang, J. Chen, P. Im, and J. DeGraw, “Grey-box modeling and application for building energy simulations-A critical review,” *Renewable and Sustainable Energy Reviews*, vol. 146, p. 111174, 2021.
- [31] F. Zapf and T. Wallek, “Gray-box surrogate models for flash, distillation and compression units of chemical processes,” *Computers & Chemical Engineering*, vol. 155, p. 107510, 2021.
- [32] O. O. Obadina, M. A. Thaha, Z. Mohamed, and M. H. Shaheed, “Grey-box modelling and fuzzy logic control of a Leader-Follower robot manipulator system: A hybrid Grey Wolf-Whale Optimisation approach,” *ISA transactions*, vol. 129, pp. 572–593, 2022.
- [33] C. Yu, L. Ljung, A. Wills, and M. Verhaegen, “Constrained subspace method for the identification of structured state-space models (COS-MOS),” *IEEE Transactions on Automatic Control*, vol. 65, no. 10, pp. 4201–4214, 2019.
- [34] M. Schoukens, “Improved initialization of state-space artificial neural networks,” in *2021 European Control Conference (ECC)*. IEEE, 2021, pp. 1913–1918.
- [35] Y. N. Dauphin and S. Schoenholz, “Metainit: Initializing learning by learning to initialize,” *Advances in Neural Information Processing Systems*, vol. 32, 2019.
- [36] M. Zakwan, L. Di Natale, B. Svetozarevic, P. Heer, C. N. Jones, and G. F. Trecate, “Physically consistent neural ODEs for learning multi-physics systems,” *arXiv preprint arXiv:2211.06130*, 2022.
- [37] L. Di Natale, B. Svetozarevic, P. Heer, and C. N. Jones, “Towards scalable physically consistent neural networks: An application to data-driven multi-zone thermal building models,” *Applied Energy*, vol. 340, p. 121071, 2023.
- [38] K. Loya, J. Buzhardt, and P. Tallapragada, “Koopman operator based predictive control with a data archive of observables,” *ASME Letters in Dynamic Systems and Control*, pp. 1–7, 2023.
- [39] J. C. Schulze and A. Mitsos, “Data-Driven Nonlinear Model Reduction Using Koopman Theory: Integrated Control Form and NMPC Case Study,” *IEEE Control Systems Letters*, vol. 6, pp. 2978–2983, 2022.
- [40] J. C. Schulze, D. T. Doncevic, and A. Mitsos, “Identification of MIMO Wiener-type Koopman models for data-driven model reduction using deep learning,” *Computers & Chemical Engineering*, vol. 161, p. 107781, 2022.
- [41] H. Choi, V. De Angelis, and Y. Preger, “Data-driven Battery Modeling based on Koopman Operator Approximation using Neural Network,” in *2023 IEEE Power & Energy Society General Meeting (PESGM)*. IEEE, 2023, pp. 1–5.
- [42] M. A. Lones, “How to avoid machine learning pitfalls: a guide for academic researchers,” *arXiv preprint arXiv:2108.02497*, 2021.
- [43] M. C. De Oliveira, J. Bernussou, and J. C. Geromel, “A new discrete-time robust stability condition,” *Systems & control letters*, vol. 37, no. 4, pp. 261–265, 1999.
- [44] M. Revay, R. Wang, and I. R. Manchester, “Recurrent equilibrium networks: Flexible dynamic models with guaranteed stability and robustness,” *IEEE Transactions on Automatic Control*, 2023.
- [45] J. Z. Kolter and G. Manek, “Learning stable deep dynamics models,” *Advances in neural information processing systems*, vol. 32, 2019.

- [46] D. Martinelli, C. L. Galimberti, I. R. Manchester, L. Furieri, and G. Ferrari-Trecate, “Unconstrained Parametrization of Dissipative and Contracting Neural Ordinary Differential Equations,” *arXiv preprint arXiv:2304.02976*, 2023.
- [47] G. Mamakoukas, O. Xherija, and T. Murphey, “Memory-efficient learning of stable linear dynamical systems for prediction and control,” *Advances in Neural Information Processing Systems*, vol. 33, pp. 13 527–13 538, 2020.
- [48] S. Bengio, O. Vinyals, N. Jaitly, and N. Shazeer, “Scheduled sampling for sequence prediction with recurrent neural networks,” *Advances in neural information processing systems*, vol. 28, 2015.
- [49] C. Yu, L. Ljung, and M. Verhaegen, “Identification of structured state-space models,” *Automatica*, vol. 90, pp. 54–61, 2018.
- [50] S. L. Brunton, J. L. Proctor, and J. N. Kutz, “Discovering governing equations from data by sparse identification of nonlinear dynamical systems,” *Proceedings of the national academy of sciences*, vol. 113, no. 15, pp. 3932–3937, 2016.
- [51] M. Chilali and P. Gahinet, “ H_2/H_∞ design with pole placement constraints: an lmi approach,” *IEEE Transactions on automatic control*, vol. 41, no. 3, pp. 358–367, 1996.
- [52] R. A. Horn and C. R. Johnson, *Matrix analysis*. Cambridge university press, 2012.
- [53] F. Zhang, *The Schur complement and its applications*. Springer Science & Business Media, 2006, vol. 4.